



RIETVELD ANALYSIS OF NANOCRYSTALLINE TITANIA PREPARED BY SOL-GEL METHOD

Emil INDREA,* Ramona-Crina SUCIU, Marcela-Corina Roșu and Teofil-Dănuț SILIPAȘ

National Institute for Research and Development of Isotopic and Molecular Technologies, 65-103 Donath,
RO-400293, Cluj-Napoca, Roumania

Received November 5, 2010

Precursor solutions for TiO₂ were prepared by the sol-gel method. The titania precursor was calcined at 450°C, 500°C, 550°C, 575°C, 600°C and 650°C. Six compositions of titania samples (sintered at different temperatures) have been taken for microstructure characterization by X-ray diffraction study using Warren–Averbach and Rietveld methods. The dominant Raman band peak positions of the 144 cm⁻¹ Eg mode in anatase TiO₂ clearly shifted to a higher values depending on the effective crystallite mean size. RDF analysis showed that at relatively small changes in the calcinations temperature of the titania precursors (575°C to 650°C), the local correlations between Ti-O and Ti-Ti atoms may suffer a significant modification.

INTRODUCTION

Nanosized materials derived from TiO₂ have been extensively investigated for vast applications, including photocatalysis, photo-catalytic effect in waste water treatment¹ and solar energy conversion.² TiO₂-based oxide systems are the most promising candidates for the development of photoelectrodes for photoelectrochemical cell (PEC) used in solar-hydrogen production.³ In our present work, we report the effect of the temperature treatment on the crystal structure and microstructure of the nanocrystalline titania prepared by sol-gel method. Rietveld analysis of the X-ray powder diffraction patterns of nanocrystalline titania was carried out in order to determine the structural and microstructural parameters.

EXPERIMENTAL

Precursor solutions for TiO₂ were prepared by the following method: tetrabutylorthotitanate (17.02 mL) and diethanolamine (4.8 mL) were dissolved in ethanol (67.28 mL). After stirring

vigorously for 2h at room temperature, a mixed solution of water (0.9 mL) and ethanol (10 mL) was added drop wise to the above solution with a burette under stirring. The resultant alkoxide solution was kept standing for 2h at room temperature for hydrolysis reaction, resulting in the TiO₂ sol. The chemical composition of the starting alkoxide solution was Ti(OC₄H₉)₄:C₂H₅OH:H₂O:NH(C₂H₄OH)₂=1:26.5:1:1 in molar ratio. The titania precursor was calcined at 450°C, 500°C, 550°C, 575°C, 600°C and 650°C.

X-ray diffraction (XRD) measurements were performed using a BRUKER D8 Advance X-ray diffractometer, working at 45 kV and 45 mA and the goniometer was equipped with a germanium monochromator in the incident beam. The X-ray diffraction patterns were collected in a step-scanning mode with steps of $\Delta 2\theta = 0.01^\circ$ using Cu K α 1 radiation ($\lambda = 1.54056 \text{ \AA}$) in the 2θ range 15–85°.

The Raman spectra were recorded in a backscattering geometry using a NRS-3300 JASCO Raman-microscope system and the 632.75 nm excitation wavelength of an Ar-ion laser, focused on a spot size of the order of $\approx 3 \mu\text{m}$.

RESULTS AND DISCUSSION

TiO₂ is known as a polymorphic material having three naturally occurring crystalline modifications, namely anatase (tetragonal; space group: I41/amd, and density = 3.9 g/cc), rutile (tetragonal, space

* Corresponding author: emil.indrea@itim-cj.ro

group: P42/mmm, density = 4.25 g/cc), and brookite (orthorhombic, space group: Pcab, density = 4.12 g/cc).⁴ All these three crystal structures are built up of TiO₆ octahedral, but in different ways. In rutile (tetragonal), two opposing edges of each octahedron are shared to form linear chains along the [0 0 1] direction, and the TiO₆ chains are linked to each other via corner connection. Anatase has no corner sharing, but has four edges shared per octahedron.⁵

Six compositions of titania samples (sintered at different temperatures) have been taken for microstructure characterization by X-ray diffraction (XRD) study using Warren–Averbach⁶ and Rietveld methods.⁷ Warren–Averbach method is a highly elaborated approach of size/strain analysis for the determination of the intrinsic physical line profile, followed by the Fourier method⁸ for evaluation of microstructural

parameters. The Rietveld method is a full-pattern fit method.⁹

XRD diffraction patterns (see Fig. 1(a)) illustrate the fact that all titania samples obtained in our synthesis conditions are multiple phase materials containing mainly the tetragonal TiO₂ anatase crystalline phase (PDF card n. 21-1272) and TiO₂ rutile crystalline phase (PDF card n. 21-1276). Rietveld method based on pseudo-Voigt profile fitting function was applied to perform a simultaneous refinement of X-ray diffraction patterns concerning both material structure and microstructure. The analysis has been done using the JAVA based software namely Materials Analysis Using Diffraction (MAUD).^{10,11} MAUD program enables a quantitative phase analysis method by comparison of the different scattering power of component materials.

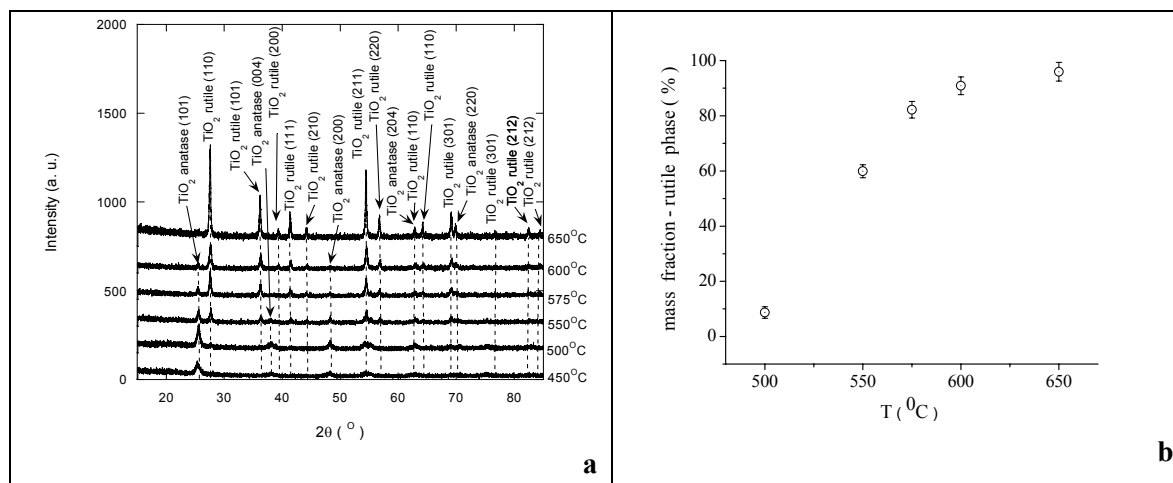


Fig. 1 – (a) The X-ray diffraction patterns of samples calcinated at 450°C, 500°C, 550°C, 575°C, 600°C, and 650°C; (b) Change of the relative proportions of anatase and rutile phase at different calcination temperatures: 500°C, 550°C, 575°C, 600°C, and 650°C.

After each thermal treatment, the percentages of anatase and rutile were calculated from X-ray powder diffraction intensities. Fig. 1(b) shows the change of the relative proportions of rutile phase at different calcination temperatures: 500°C, 550°C, 575°C, 600°C, and 650°C. The anatase phase decreases and the rutile phase increases with increasing calcination temperature. When the calcinations temperature increases up to 650°C, the anatase transformation into rutile was complete.

Microstructural informations obtainable by the X-ray Rietveld refinement method consist of effective crystallite mean size, D_{eff} (nm) and the root mean square (rms) of the microstrains averaged along the $[hkl]$ direction, $\langle \varepsilon^2 \rangle^{1/2}_{hkl}$.¹² The microstructural parameters, profile (Rp) and

weighted profile (Rwp) discrepancy indices at their reached minimum values are presented in the Table 1.

Fig. 2(a) shows the crystallite size D_{eff} and Fig. 2(b) shows the root mean square microstrain $\langle \varepsilon^2 \rangle^{1/2}$ (isotropic) of the titania-rutile samples calcined at 500°C, 550°C, 575°C, 600°C, and 650°C.

The microstructural parameters of nanostructured titania showed an increase in the average size of the rutile particles from 40 nm (rutile nascent phase) to 95 nm for photocatalysts nanocrystals calcined above 550°C. The lattice microstrain $\langle \varepsilon^2 \rangle^{1/2}$ of the titania calcinated at 500°C has a very high values due to growth mechanism of the nascent rutile phase.

Table 1

The microstructural parameters D_{eff} (nm), $\langle \varepsilon^2 \rangle^{1/2}_{\text{hkl}}$, profile (Rp) and weighted profile (Rwp) discrepancy indices obtained by the X-ray Rietveld refinement method for the titania-rutile investigated samples

Samples	Temperature treatment ($^{\circ}\text{C}$)	D_{eff} (nm)	$\langle \varepsilon^2 \rangle^{1/2}_{\text{hkl}} \times 10^3$	Rp	Rwp
TR500	500	43	19.67	10.4	12.6
TR550	550	50	3.93	8.8	10.8
TR575	575	55	1.48	7.2	8.8
TR600	600	64	0.64	7.4	9.2
TR650	650	96	0.56	8.6	10.4

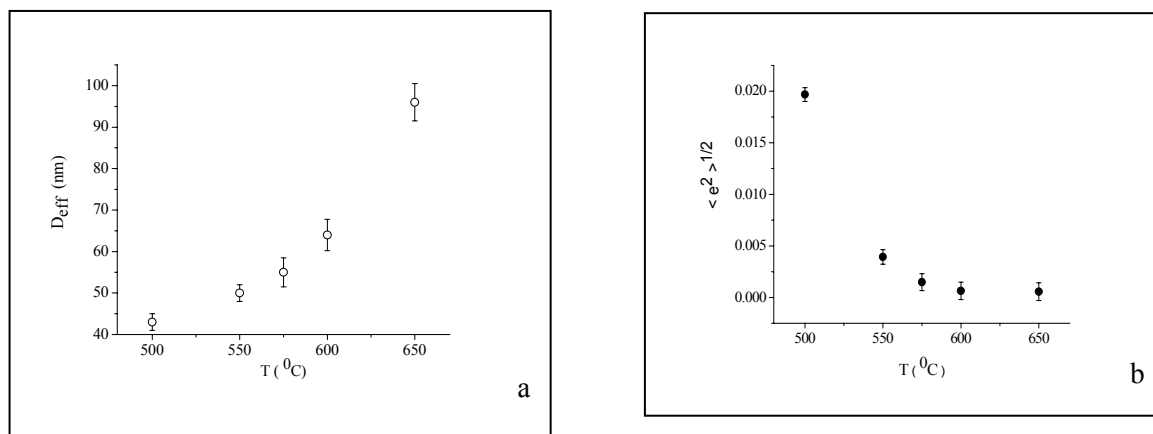


Fig. 2 – (a) The titania-rutile effective crystallite size D_{eff} and (b) the root mean square microstrain $\langle \varepsilon^2 \rangle^{1/2}$ of the titania-rutile calcined at 500 $^{\circ}\text{C}$, 550 $^{\circ}\text{C}$, 575 $^{\circ}\text{C}$, 600 $^{\circ}\text{C}$, and 650 $^{\circ}\text{C}$.

The lattice microstrain shows a decreasing value in the intercrystallite zones that suggests an anatase-rutile phase decreasing interaction for photocatalysts nanocrystals calcined above 500 $^{\circ}\text{C}$. The titania nanoparticles are aggregated in the nascent rutile phase for nanocrystals calcined above 650 $^{\circ}\text{C}$.

The typical disorder B-factor estimated from the X-ray diffraction data estimates the average displacement of an atom around the centroid of distinct atomic positions in different unit cells.

Fig. 3(a) shows isotropic B factors for Ti atoms and Fig. 3(b) shows isotropic B factors for O atoms

of the titania-rutile samples calcined at 500 $^{\circ}\text{C}$, 550 $^{\circ}\text{C}$, 575 $^{\circ}\text{C}$, 600 $^{\circ}\text{C}$, and 650 $^{\circ}\text{C}$, calculated using the MAUD software. The atomic local disorder of Ti and O atoms shows an decreasing value in rutile phase of the nanocrystals calcined above 500 $^{\circ}\text{C}$.

The Raman spectra of the titania powder obtained by the temperature treatment of the precursor solution at 450 $^{\circ}\text{C}$, 500 $^{\circ}\text{C}$, 550 $^{\circ}\text{C}$, 575 $^{\circ}\text{C}$, 600 $^{\circ}\text{C}$ and 650 $^{\circ}\text{C}$, respectively, are shown in Fig. 4, using a wavelength of $\lambda=632.75$ nm.

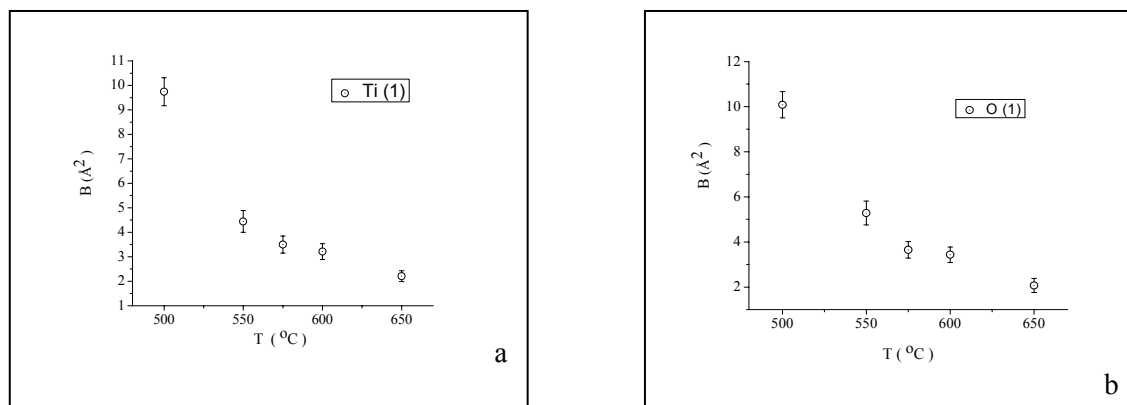


Fig. 3. (a) Isotropic B factors for Ti atoms and (b) Isotropic B factors O atoms of the titania samples calcined at 500 $^{\circ}\text{C}$, 550 $^{\circ}\text{C}$, 575 $^{\circ}\text{C}$, 600 $^{\circ}\text{C}$, and 650 $^{\circ}\text{C}$.

From Fig. 4, the frequencies of Raman bands identified as $143.4 (\pm 2.8) \text{ cm}^{-1}$ are assigned to the E_g phononic modes represented by ν_6 . The bands as $397.1 (\pm 4.3) \text{ cm}^{-1}$ are assigned to the $B1g$ phononic mode (ν_4). The bands as $516.4 (\pm 5.3) \text{ cm}^{-1}$ can be attributed to the $A1g$ phononic mode (ν_2). The bands as $513.14 (\pm 7.4) \text{ cm}^{-1}$ can be attributed to the $B1g$ phononic mode (ν_3), and the bands as $639.4 (\pm 10.2) \text{ cm}^{-1}$ can be attributed to the E_g phononic mode (ν_1), based on the factor group analysis.¹³ The frequencies of Raman bands identified as $A1g$ (610 cm^{-1}), $B1g$ (143 cm^{-1}), $B2g$ (830 cm^{-1}) and Eg (448 cm^{-1}) can be attributed to the rutile tetragonal phases of titanium dioxide TiO_2 .¹³

These bands agree well with those in previous studies for anatase powder and rutile tetragonal phases of titanium dioxide.¹⁴ From the factor plane analysis it was observed that both $A1g$ (ν_3) and $B1g$ (ν_2) modes involve the Ti-O bond stretching.¹⁵ The positions and widths of the major peaks are all shifted with respect to the corresponding frequencies in the bulk material. In our previous work on anatase TiO_2 nanocrystalline powders, we studied the changes that appear in the Raman spectra with the increase of the treatment temperature nanocrystalline titania, concerning especially line widths of the 144 cm^{-1} band in terms of finite-size effect of nanocrystallinity.¹⁶

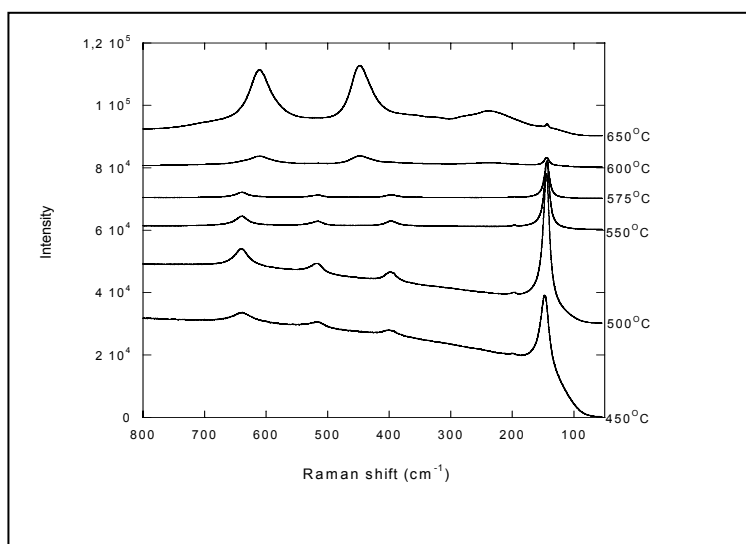


Fig. 4 – Raman spectra of a nanocrystalline titania nanocrystals calcined at 450°C, 500°C, 550°C, 575°C, 600°C and 650°C.

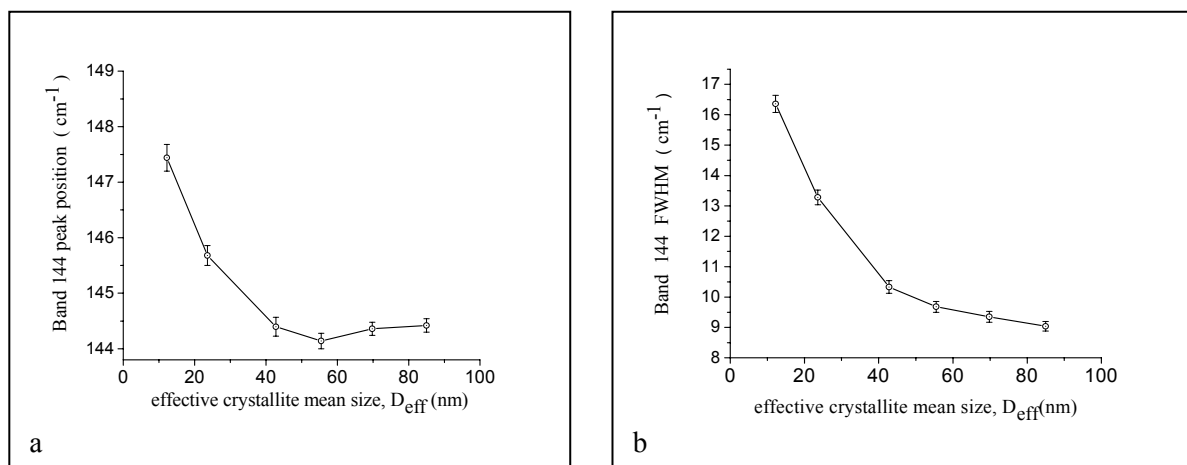


Fig. 5 – (a) Raman 144 cm^{-1} band peak positions (cm $^{-1}$) vs. effective crystallite mean size, D_{eff} (nm); (b) Raman 144 cm^{-1} band peak width (FWHM) vs. effective crystallite mean size, D_{eff} (nm).

The peak positions and widths were determined by spectral deconvolution. Raman band peak positions (cm^{-1}) and band peak widths (FWHM) of the 144 cm^{-1} Raman band vs. effective crystallite mean size, $D_{\text{eff}}(\text{nm})$ are drawn on Fig. 5(a)-(b). Similar shifts have been previously reported and have been related to the confinement effects in nanostructured anatase crystallites.¹⁷ The dominant 144 cm^{-1} Eg mode in anatase TiO_2 clearly shifted to a higher value by $0.45\text{--}5.7 \text{ cm}^{-1}$ depending on the effective crystallite mean size (shown in Fig. 5(a)). In addition, as shown clearly in Fig. 5(a), and Fig. 5(b) for the 144 cm^{-1} Eg line, as the shift increases, so does the line broadening, which indicates that the strain field within the titania crystallites volume is rather inhomogeneous, but that this inhomogeneity decreases as the the grain size increases and the rmc decreases.

Detailed information calculated through Rietveld refinement using the MAUD software

about the atomic coordinate type (e.g. Cartesian or fractional) has been used to compute three-dimensional structural model as the Radial Distribution Functions $g(r)$ (RDF)¹⁸ by a computer program named ISAACS (interactive structure analysis of amorphous and crystalline systems).¹⁹

Results of the calculation of the radial distribution functions RDF for a 3000-atom model of titania (see Fig. 6) exhibits a first sharp peak positioned at 2.2 \AA , which is the Ti-O distance in and a second RDF peak, at 3.6 \AA , that reflects the correlations between Ti atoms. RDF analysis showed that at relatively small changes in the calcinations temperature of the titania precursors (575°C to 650°C), in which case the rutile phase is predominant, the local correlations between Ti-O and Ti-Ti atoms are may suffer a significant modification.

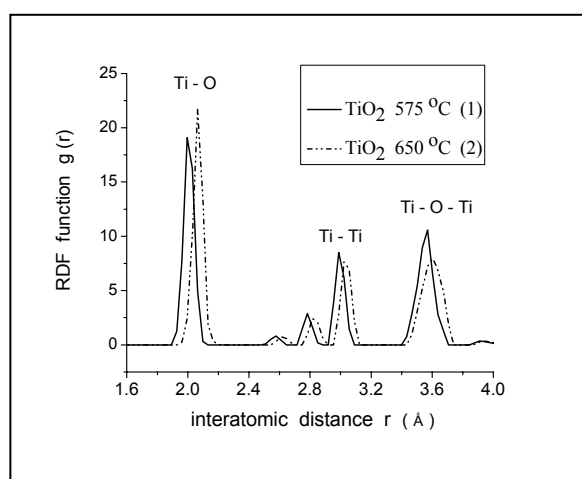


Fig. 6 – RDF function for a 3000-atom model of titania that reflects the correlations between Ti-O and Ti-Ti atoms in the titania samples calcined at 575°C and 650°C .

CONCLUSIONS

Rietveld refinement of powder X-ray diffraction of titania precursors calcined at 450°C , 500°C , 550°C , 575°C , 600°C and 650°C were undertaken to obtain structural data (lattice parameters and position coordinates) and microstructural data (crystallinity, and strain).

The microstructural parameters of nanostructured titania showed an increase in the average size of the rutile particles from 40 nm (rutile nascent phase) to 95 nm for photocatalysts nanocrystals calcined above 550°C . The lattice microstrain $\langle \epsilon^2 \rangle^{1/2}$ of the titania calcinated at 500°C has a very high values due to growth mechanism of the nascent rutile phase. The titania nanoparticles are

aggregated in the rutile phase for nanocrystals calcined above 650°C .

Detailed information calculated through Rietveld refinement using the MAUD software about the atomic coordinate type (e.g. Cartesian or fractional) has been used to compute three-dimensional structure model as the Radial Distribution Functions $g(r)$ (RDF). RDF for a 3000-atom model of titania reflects the correlations between Ti-O and Ti-Ti atoms in the titania calcined samples.

Acknowledgements: This work was supported by the Roumanian Ministry of Education and Research through the project INCDTIM Cluj-Napoca, PN 09-44 02 06.

REFERENCES

1. Xiaobin Li, Linling Wang and Xiaohua Lu, *J Hazard Mater*, **2010**, 177, 639-647.
2. H Tributsch, *Int J Hydrogen Energy*, **2008**, 33, 5911-5930.
3. J. Nowotny, C.C. Sorrell, L.R. Sheppard and T. Bak, *Int. J. Hydrogen Energy*, **2005**, 30, 521-544.
4. V. Petkov, *J. Appl. Crystallogr.*, **1989**, 22, 387-392.
5. A. Di Paola, G. Cufalo, M. Addamo, M. Bellardita, R. Campostrini, M. Ischia, R. Ceccato and L. Palmisano, *Colloid Surfaces A*, **2008**, 317, 366-376.
6. B.E. Warren and B.L. Averbach, *J. Appl. Phys.*, **1950**, 21, 595-599.
7. H.M. Rietveld, *J. Appl. Cryst.*, **1969**, 2, 65-73.
8. J.G.M. van Bercum, A.C. Vermeulen, R. Delhez, T.H. de Keijser and E.M. Mittemeijer, *J. Appl. Phys.*, **1994**, 27, 345-353.
9. L. Lutterotti and P. Scardi, *J. Appl. Crystallogr.*, **1990**, 23, 246-253.
10. L. Lutterotti, P. Scardi and P. Maistrelli, *J. Appl. Crystallogr.*, **1992**, 25, 459-465.
11. L. Lutterotti, MAUD Version 2.062, <http://www.ing.unitn.it/~maud/> **2007**.
12. E. Indrea and A. Barbu, *Appl. Surf. Sci.*, **1996**, 106, 498-501.
13. A. Ibrahim, A. Alhomoudi and G. Newaz, *Thin Solid Films*, **2009**, 517, 4372-4378.
14. G. Gu, Y. Li, Y. Tao, Z. He, J. Li, H. Yin, W. Li and Y. Zhao, *Vacuum*, **2003**, 71, 487-493.
15. W. X. Xu, S. Zhu, X.C. Fu and Q. Chen, *Appl. Surf. Sci.*, **1999**, 148, 253-258.
16. L. Baia, A. Peter, V. Coşoveanu, E. Indrea, M. Baia, J. Popp and V. Danciu, *Thin Solid Films*, **2006**, 511-512, 512-516.
17. N. Mahdjoub, N. Allen, P. Kelly and V. Vishnyakov, *J Photoch Photobio A*, **2010**, 211, 59-64.
18. Ke-Rong Zhu, M.-S. Zhang, Q. Chen and Z. Yin, *Physics Letters A*, **2005**, 340, 220-227.
19. M. Allen and D. Tildesley, "Computer Simulation of Liquids", Oxford Science Publications, 1987.